

Direct Fabrication of Cobalt Oxide Nano-particles Employing Glycine as a Combustion Fuel

M. Th. Makhoulf, B. M. Abu-Zied*, T. H. Mansoure

Chemistry Department, Faculty of Science, Assiut University, 71516, Assiut, Egypt

Abstract Combustion method has been used as a fast and facile method to prepare nanocrystalline Co_3O_4 spinel employing glycine as a combustion fuel. The products were characterized by thermal analyses (TGA & DTA), X-ray diffraction technique (XRD), Fourier transform infrared spectroscopy (FTIR), Scanning electron microscopy (SEM), and Transmission electron microscopy (TEM) techniques. Experimental results revealed that the molar ratio of fuel/oxidant play an important role in controlling the crystallite size of Co_3O_4 nanoparticles. Transmission electron microscopy indicated that the crystallite size of Co_3O_4 nanocrystals were in the range of 14–31 nm. Since the particle size of the powdered samples were found to be equivalent from both TEM and X-ray diffraction technique. X-ray diffraction confirmed the formation of CoO phase with spinel Co_3O_4 . The effect of calcination temperature on crystallite size and morphology has been discussed.

Keywords Nanao-materials, Nano-crystalline Co_3O_4 , Combustion Synthesis, Cobalt Oxide

1. Introduction

Transition metal oxides have attracted the attention of scientific researchers due to their promising applications in various fields. Among of these metal oxides cobalt oxide Co_3O_4 , one of the most active catalyst for the total oxidation of methane¹. Cobalt oxide has a wide range of applications in N_2O decomposition, oxidation of volatile organic compounds (VOCs), Fischer-Tropsch synthesis (FTS), steam reforming of ethanol, low temperature CO oxidation, and hydrogen peroxide decomposition²⁻⁷. It is well known that the properties of Co_3O_4 catalyst are strongly depending on its shape and size. Co_3O_4 with nanosized have high surface area is expected to lead to even more attractive applications in conjunction of their traditional arena and nanotechnology⁸. Therefore, it is important to prepare Co_3O_4 with defined morphologies and a narrow range of size distribution. Much effort has been made to synthesize Co_3O_4 catalyst from economical and practical aspects point of view including micro-emulsion, thermal decomposition of cobalt oxalate, one-pot hydrothermal reaction, and sol-gel⁹⁻¹². In addition, there are some reports involving the synthesis of Co_3O_4 nanocrystallites with various morphologies. For instance, Co_3O_4 crystallites with different morphologies such as urchin, spherical and quasi-cubic morphology were obtained by soft chemical method¹³. Co_3O_4 nanocubes were prepared by hydrothermal oxidation method¹⁴. Co_3O_4

nanorods were synthesized by molten salt approach¹⁵. Sphere-like Co_3O_4 nanocrystals was synthesized by simple polyol route¹⁶, and combustion method using urea as a fuel¹⁷.

In recent years, combustion synthesis (CS) or self-propagating high-temperature synthesis (SHS) has been used as a facile technique for preparation of catalysts, alloys, composites and nanomaterials. CS is classified into two groups, depending upon the nature of reactants: (i) solid state combustion (SSC), and (ii) solution combustion synthesis (SCS). In SSC, initial reactants, intermediates and final products are all in the solid state. The disadvantages of this method are that the heterogeneity for the initial solid reactants is on the order of 10-100 μm . This feature, coupled with high reaction temperatures ($>2000\text{ K}$), makes it difficult to synthesize nanosize structures with high surface area¹⁸. SCS has emerged as an effective, fast, simple and low cost method for synthesize of a variety of nanosize materials. This process involves self-sustained reaction in homogeneous solutions of metal nitrates (oxidizer) and fuels (i.e., glycine, citric acid, urea ... etc.). It yield homogenous, crystalline, and high-purity product. Glycine has been used as a fuel to synthesize different nanomaterials¹⁹⁻²¹. Grover et al. have prepared nanocrystalline ceria-doped-zirconia powder using glycine as a fuel¹⁹. The calcined powders showed the presence of regular particles, with narrow particle size distribution. Deraz has demonstrated that when glycine alone is used as a fuel, nanosized CoFe_2O_4 is formed with CoO ²⁰. Zavyalova et al. have studied the effect of using different fuels on catalytic activity of nanosized $\text{Co}_3\text{O}_4/\gamma\text{-Al}_2\text{O}_3$ catalysts for the total oxidation of methane¹. The obtained results showed that, the catalysts synthesized from equimolar redox mixtures such as cobalt nitrate/

* Corresponding author:

babuzied@aun.edu.eg (B. M. Abu-Zied)

Published online at <http://journal.sapub.org/pc>

Copyright © 2012 Scientific & Academic Publishing. All Rights Reserved

glycine or cobalt acetate/cobalt nitrate exhibited the highest activity.

In the present work, we report a facile, convenient, fast, and inexpensive method to prepare Co_3O_4 nanoparticles via SCS using glycine as a combustion fuel and cobalt nitrate as oxidizer. Our investigation studies the effect of fuel to oxidant molar ratios (F/O) as well as the calcination temperature in controlling particle size and morphology of prepared Co_3O_4 . The textural and structure properties of the prepared Co_3O_4 nano-particles were characterized by means of thermal analyses (TGA & DTA), X-ray powder diffraction (XRD), Fourier transform infrared spectroscopy (FT-IR), and electron microscopy (SEM & TEM).

2. Experimental

2.1. Preparation Procedure

Cobalt nitrate, $\text{Co}(\text{NO}_3)_2 \cdot 6\text{H}_2\text{O}$, and glycine, $(\text{NH}_2\text{CH}_2\text{COOH})$, were of analytical grade reagents and were used without further purification. Distilled water was used in all of preparations. A schematic representation of the synthesis procedure used in the synthesis of nano-crystalline Co_3O_4 is schematically shown in Fig. 1. Two series of samples were prepared. In the first one (series I) we have investigated the effect of changing the glycine/cobalt molar ratios (F/O), 0.5, 1, 1.5, 2, 5, 8 and 16 on the morphology and crystallite size of Co_3O_4 . In a typical procedure, the required amounts of cobalt nitrate and glycine were weighed to the nearest milligram. Cobalt nitrate and glycine were dissolved in 100 ml of distilled water to form a pink homogeneous solution; the solution was then heated on a hotplate at about 100°C to evaporate the excess water. After that the obtained viscous gel were calcined in muffle furnace at 400°C for 3h in a static air atmosphere. In series II, we have investigated the effect of changing the calcinations temperature, $350\text{--}1000^\circ\text{C}$ employing the same procedure and a glycine/cobalt molar ratio of 0.5.

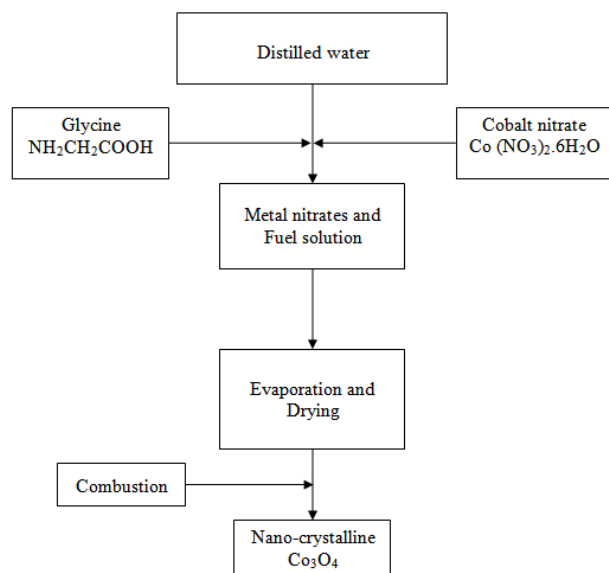


Figure 1. A schematic representation of the synthesis process

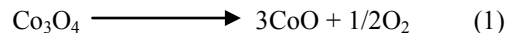
2.2. Characterization

Simultaneous TGA and DTA curves were recorded with a shimadzu DTG-60 instrument apparatus using a heating rate of $10^\circ\text{C min}^{-1}$ in air atmosphere (flow rate 40 ml/min). Powder X-ray diffraction (XRD) patterns were recorded using Philips diffractometer (type PW 103/00) with $\text{CuK}\alpha$ radiation ($\lambda = 1.5405\text{ \AA}$) at 35 kV and 20 mA with a scanning rate in 2θ of 0.06 min^{-1} . FTIR spectra were performed employing the KBr disc technique in the wavelength range $4000\text{--}400\text{ cm}^{-1}$, using Thermo-Nicolet-6700 FTIR spectrophotometer. Scanning electron micrographs were obtained using a JEOL scanning microscope (model JSM-5400 LV). Transmission electron pictures were taken using JEOL transmission microscope (model JEMTH-100 II).

3. Results and Discussion

3.1. Thermal Analysis

Fig.2 shows the weight loss (TG) and the associated derivative thermogram (DTG) of the precursor synthesized at F/O equal 0.5 in air atmosphere as a carrier gas. This figure manifests that the precursor underwent four-step decomposition with increasing the temperature from ambient till 915°C . The first step starts from room temperature till around 145°C which brings a weight loss (WL) of 27 %. This step can be ascribed to dehydration, deamination, starting of decarboxylation, and denitration of the precursor. The second step exhibits a weight loss of 27.4 %, within a narrow temperature range $145\text{--}190^\circ\text{C}$. It can be associated to simultaneous melting of the precursor and continuous denitration of remaining nitrates coming from cobalt precursor. The third step at 260°C with a weight loss of 9 % could be attributed to the complete decomposition of the precursor and formation of spinel Co_3O_4 . Further heating the precursor up to 1000°C , one can observe the fourth step at 915°C . This step is accompanied by weight loss of 2.5 % due to the decomposition of Co_3O_4 into CoO [2] according to the following equation:



The inserted curves in Fig.2 shows a magnification of both the heating and the cooling curves of the precursor at the 800°C till 1000°C temperature range. It illustrates that the cooling of CoO phase formed at 915°C , as a product of the decomposition of spinel Co_3O_4 phase, has a weight gain of 2.5 %. This weight gain could be attributed to the oxidation of CoO into Co_3O_4 , and this in turn, indicates the reversibility of the above equation. It is worth to noting that, in case of lower fuel/oxidant molar ratio (i.e. 0.5) a multi-step decomposition of precursor was observed. On increasing the F/O to a value of two the obtained thermogram (not shown) these multistep processes emerged only as a single WL step.

Fig. 3 shows the obtained DTA curve during heating the precursor with F/O molar ratio of 0.5 in air atmosphere till 1000°C . Inspection of this figure reveals the presence of

distinct two-endothermic peaks at the 25-92°C temperature range. Such effects could be related to the dehydration of the precursor. In addition, the thermogram shows a sharp exothermic peak at 141°C. The temperature of such peak is consistent with that of the first WL step observed in the TGA pattern. This effect corresponds to simultaneous evolving of NO_3^- and glycine. Simultaneously, glycine is oxidized by nitrate anions (resulting carbon dioxide, nitrogen, nitrogen dioxide and water²²) releasing plenty of gases. Thus, the exothermic peak could be attributed to the combustion of evolved gases. The narrow endothermic peak at 194°C associated with the second WL step in TGA. This endothermic peak related to melting of the precursor and simultaneously, continuous decomposition of cobalt nitrate hexahydrate. It is well known that, combustion consist of

three components namely fuel, oxidizer and ignition temperature. Fuel is capable of burning by braking C-H bonds or gaining electrons from the oxidizer. Insufficient fuel will make the combustion process incomplete. Thus, the observed endothermic peak corresponds to the melting and continuous decomposition of the precursor. In this context, DTA of the precursor with F/O of 2 did not show this endothermic effect (as shown in Fig. 4). The observed exothermic peak at 263°C corresponds to complete decomposition of the precursor and crystallization of Co_3O_4 spinel. Going to the high temperature range the obtained DTA thermogram manifests the presence of an endothermic peak at 915°C. Such effect can be ascribed to the decomposition of Co_3O_4 into CoO^2 , i.e. thermal reduction of Co^{3+} to Co^{2+} .

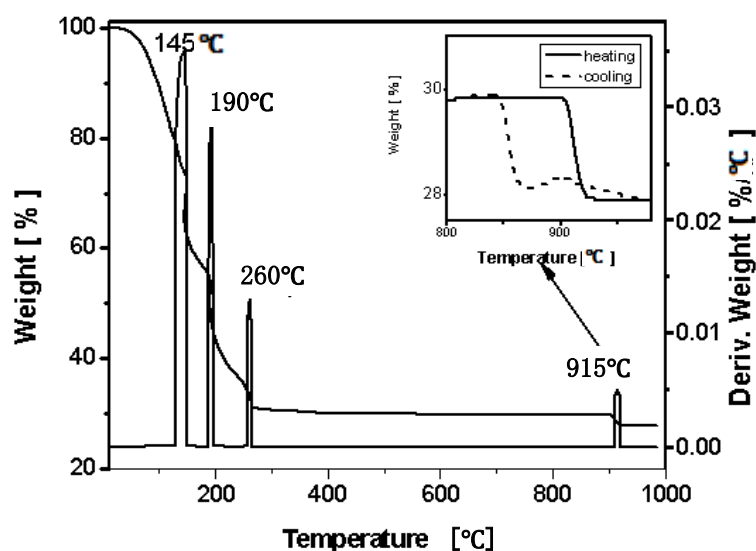


Figure 2. TGA and DTG curves obtained by heating the precursor having F/O ratio of 0.5 in air atmosphere

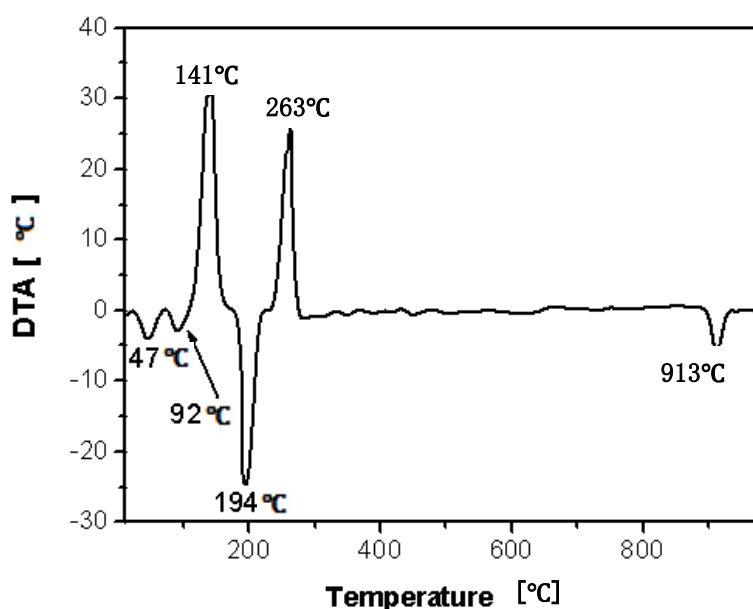


Figure 3. DTA thermogram obtained by heating the precursor (F/O equal 0.5) in air atmosphere

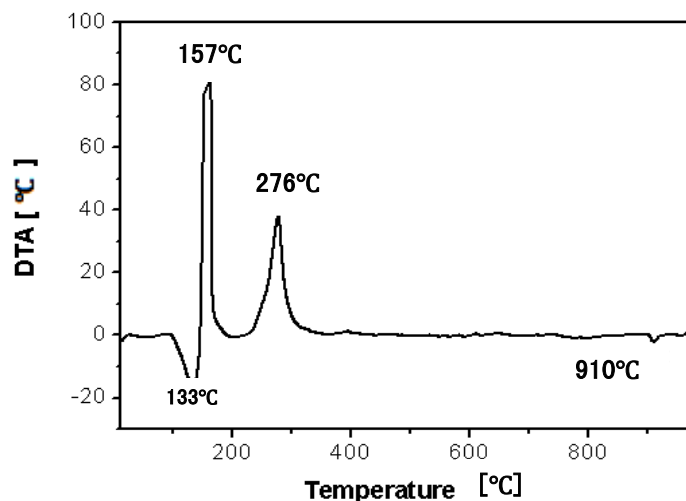


Figure 4. DTA thermogram obtained by heating the precursor (F/O equal 2) in air atmosphere

3.2. X-ray Diffraction

X-ray diffraction (XRD) patterns of the as-prepared Co_3O_4 obtained via combustion synthesis at different glycine/cobalt molar ratios (i.e. 1, 1.5, 2, 5, 8, and 16) being calcined at 400 °C are shown in Fig. 5 (curves a-g). Inspection of this figure revealed that: (i) When the F/O molar ratio is 0.5 and 1 (patterns a and b, respectively) the powder after combustion contain only well crystallized cubic spinel Co_3O_4 (JCPDS card file No. 80-1545). (ii) When the molar ratio in the range 1.5-5 (patterns c-e), the powders is composed of a mixture of Co_3O_4 and CoO (JCPDS 78-0431). (iii) When the molar ratio more than 5, again the powder diffraction patterns are composed only Co_3O_4 as in pattern f and g. In other words, with increasing the glycine/cobalt molar ratio, the amount of Co_3O_4 decreased whereas that of CoO increased (i.e. the intensities of the peaks related to Co_3O_4 are lowered and that of CoO are increased). The amount of CoO reached its maximum value at molar ratio of 2, after that, with further increase in the F/O ratio the molar ratio the amount of CoO decreased and that of Co_3O_4 increased again. At molar ratio of 8, the peaks related to CoO disappeared as shown in Fig. 5-f. In this context, Deraz²⁰ have prepared nanosized CoFe_2O_4 phase with a minor amount of CoO, when using glycine alone as a fuel. Thus, combustion synthesis using glycine is proposed to be a route to synthesis reduced oxidation state compounds such as CoO phase²⁰.

In order to check the role of glycine molar ratio in changing the structural parameters of Co_3O_4 such as lattice parameter (a) and crystallite size (D). The lattice parameters were computed using the *d*-spacing values and the respective (hkl) parameters. The obtained results are plotted in Fig. 6-a. The crystallite size (D) was calculated using scherrer equation²¹ from the full-width at half-maximum (FWHM) of the peaks. The relevant values are listed in table 1. From table 1, it is evident that the crystallite size of Co_3O_4 increased with increasing the glycine/cobalt molar ratio till a value of 5, and then it shows a mild decrease upon further F/O increase. This in turn indicates that, the lower

glycine/cobalt value the smaller the Co_3O_4 crystallite size. Fig. 6-a shows the effect of the molar ratio variation on the lattice parameter of Co_3O_4 . It is obvious that the variation of the lattice parameter with molar ratio follows the same trend as that observed for the crystallite size, i.e. lower molar ratio value leads to lower lattice parameter. Accordingly, one can state safely that the obtained nano-scaled Co_3O_4 samples by SCS are attributed to two factors: (i) first, the reactants are mixed in the liquid state, which allows the uniform distribution of the reactants at atomic or molecular levels. (ii) Second, the high temperature of combustion reaction and short reaction time, which enable the formation and evolution of various gases that inhibit the growth of particle size and formation of nano-sized Co_3O_4 .

Since the Co_3O_4 obtained by using a molar ratio of 0.5 exhibits the lowest crystallite size, the study was extended to check the influence of changing the calcination temperature on the morphology and crystallite size of Co_3O_4 at this ratio. XRD patterns of the as-prepared Co_3O_4 obtained via calcining glycine/cobalt parents having molar ratio of 0.5 at 350-1000°C temperature range are shown in Fig. 7 a-h. From this figure two points could be raised: (i) all diffraction peaks belong to one phase only (Co_3O_4), and (ii) No diffraction peaks related to CoO appear even at high temperatures (i.e. 900 or 1000°C) indicating that the final product of high purity. This is in a good agreement with the thermal analysis results (Fig. 2) by confirming the reversibility of equation 1, i.e. CoO when formed at high temperature it spontaneously converted to Co_3O_4 on cooling. Table 2 gives the average crystallite size of Co_3O_4 phase at different calcination temperatures (350-1000°C) calculated from XRD data, whereas the relevant lattice parameters are shown in Fig. 6-b. From these data one can state safely that, the sample calcined at 400°C exhibits the lowest average crystallite size (*D* = 15.3 nm). With increasing the calcination temperature the average crystallite size is also increased. Accordingly, the optimum conditions to obtain pure Co_3O_4 with smallest crystallite size using glycine as a fuel is glycine/cobalt ratio of 0.5 and a calcination temperature at 400°C.

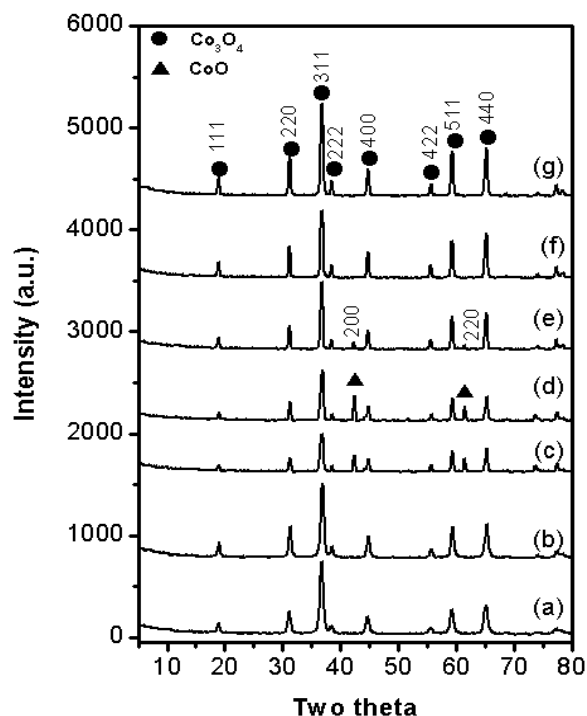


Figure 5. XRD patterns of nano-crystalline Co_3O_4 samples calcined at 400°C , being prepared at different glycine/cobalt nitrate molar ratios; (a) 0.5, (b) 1, (c) 1.5, (d) 2, (e) 5, (f) 8, and (g) 16

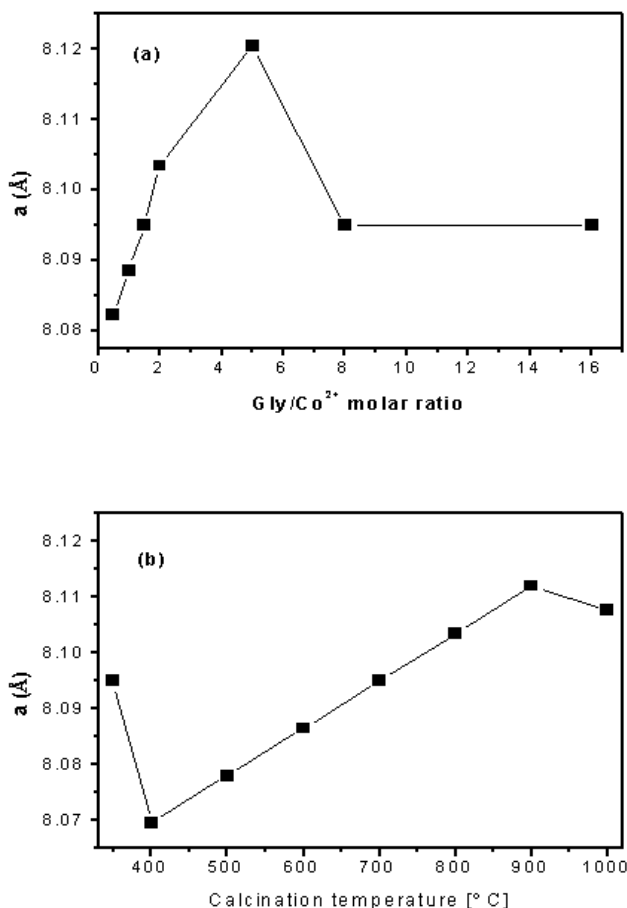


Figure 6. Fig. 6: Effect of glycine to cobalt nitrate ratios (a) and calcination temperature (b) on the lattice parameter values of nano-crystalline Co_3O_4

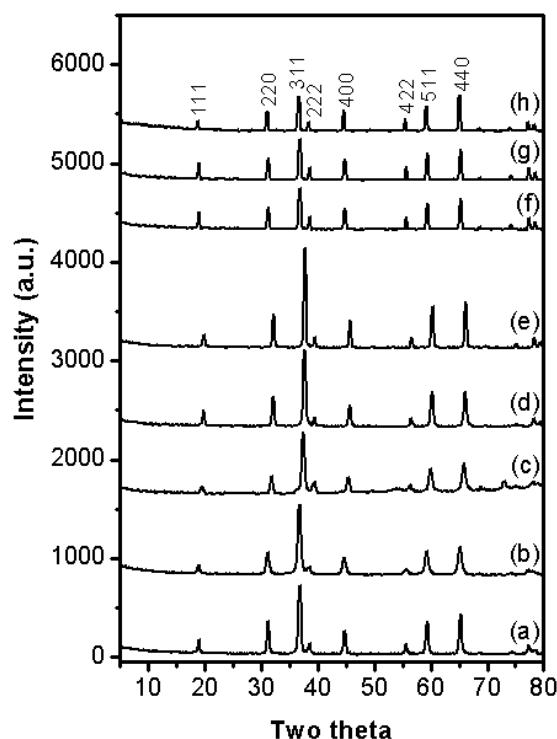


Figure 7. XRD patterns of nano-crystalline Co_3O_4 samples obtained via glycine/cobalt nitrate molar ratio of 0.5 at different calcinations temperature; (a) 350°C , (b) 400°C , (c) 500°C , (d) 600°C , (e) 700°C , (f) 800°C , (g) 900°C , and (h) 1000°C

3.3. Infrared Spectra

Cubic spinel structure of Co_3O_4 with Co^{2+} ($3d^7$) and Co^{3+} ($3d^6$) located at tetrahedral and octahedral sites, respectively, belongs to the space group ($Fd3m$)¹⁶. The group theory predicts the following modes in the spinel²³: $\Gamma = A_{1g}(\text{R}) + E_g(\text{R}) + F_{1g}(\text{in}) + 3F_{2g}(\text{R}) + 2A_{2u}(\text{in}) + 2E_u(\text{in}) + 4F_{1u}(\text{IR}) + 2F_{2u}(\text{in})$, where (R), (IR) and (in) represent Raman active vibrations, infrared-active vibration and inactive modes, respectively. The FT-IR spectra of as-prepared nanocrystalline Co_3O_4 at different F/O molar ratios being calcined at 400°C are shown in Fig. 8 (curves a-g). In the investigated region ($4000\text{--}400\text{ cm}^{-1}$), the entire obtained spectra manifest the presence of two absorption bands at $576(\nu_1)$ and $661(\nu_2)\text{ cm}^{-1}$; which originate from the stretching vibrations of the metal-oxygen bond and confirm the formation of Co_3O_4 spinel oxide². The ν_1 band is characteristic of OB_3 (where B denotes the Co^{3+} in the octahedral hole) vibration and the ν_2 band is attributable to the ABO_3 (where A denotes the Co^{2+} in the tetrahedral hole) vibration in the spinel lattice. In addition, the intensities of the peaks are decreased and become broader with increasing F/O value. Also, the FT-IR spectra show no residual organic compounds and NO_3^- after calcinations. It is worth noting that, it is very difficult to differentiate between the FT-IR spectra of pure Co_3O_4 and that of Co_3O_4 with CoO impurities. Thus the presence of some CoO impurities in the Co_3O_4 nanoparticles cannot be excluded based on analysis of FT-IR only. The FTIR spectra of nano-crystalline Co_3O_4 samples having F/O 0.5 being calcined at $350\text{--}1000^\circ\text{C}$ temperature range (not shown), Also exhibit two bands at $576(\nu_1)$ and

668 (ν_2) cm^{-1} ; which originate from the stretching vibrations of the cobalt-oxygen bond and confirm the formation of Co_3O_4 spinel oxide.

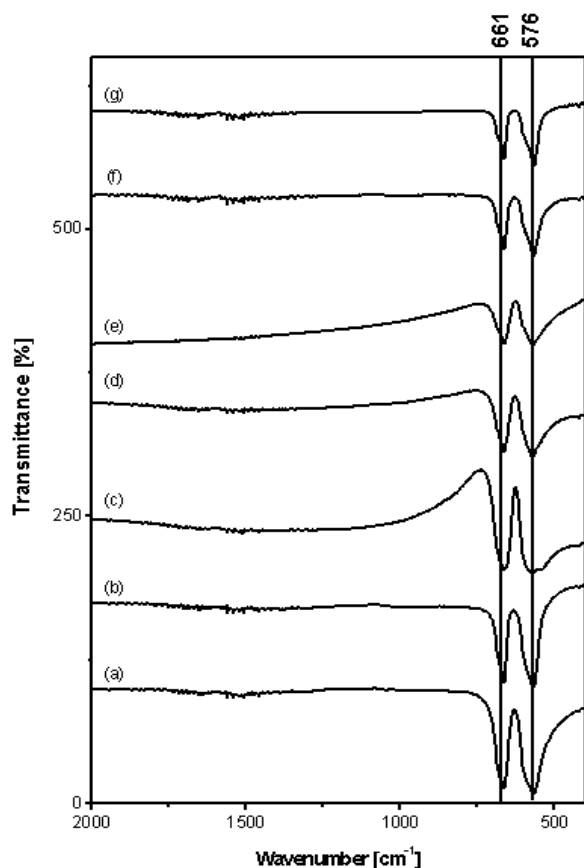


Figure 8. FTIR spectra of as-prepared nano-crystalline Co_3O_4 at different molar ratios of glycine to cobalt nitrate; (a) 0.5, (b) 1, (c) 1.5 (d) 2, (e) 5, (f) 8, and (g) 16

3.4. Electron Microscopy (SEM&TEM)

The SEM micrographs of the synthesized Co_3O_4 calcined at 400°C for F/O ratios of 1 and 5 are shown in Fig. 9-a and -b, respectively. Inspection of this figure manifests that the

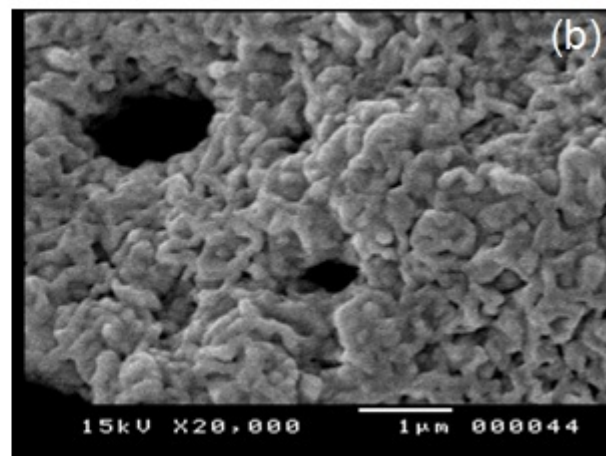
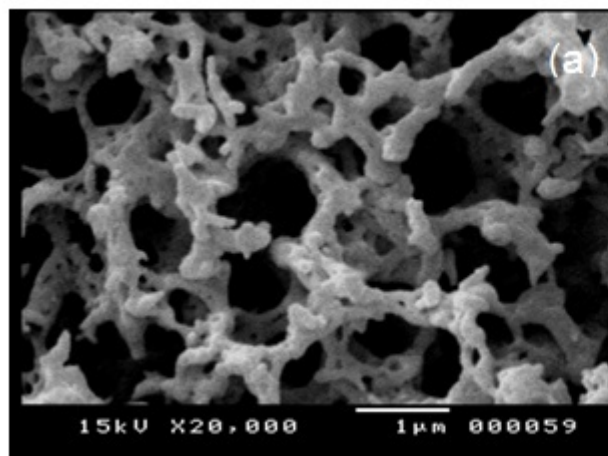


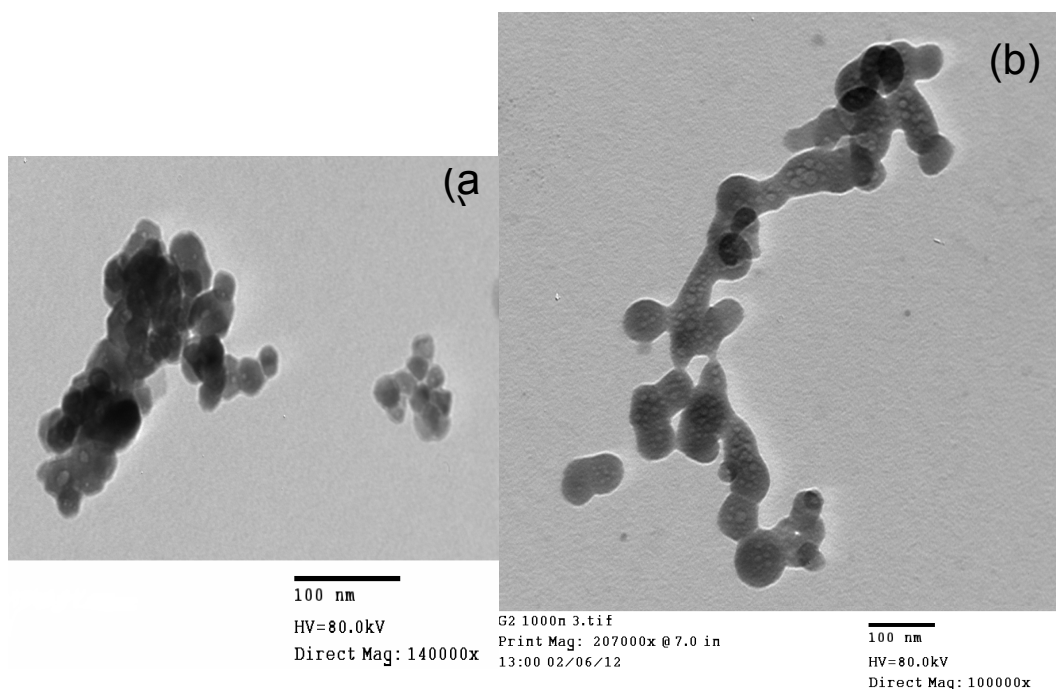
Figure 9. SEM of as-prepared Co_3O_4 at different glycine to cobalt molar ratios, (a) 1, (b) 5, being calcined at 400°C

prepared spinel Co_3O_4 shows a porous network as a consequence of the gases escaping during the combustion process. Moreover, it is obvious that the nano-particles are uniform hollow tubular shapes with voids and holes randomly distributed among them. Particles of Co_3O_4 are agglomerated regardless of the F/O molar ratio but the degree of agglomeration is increased with increasing F/O molar ratio. It is clear that, the lower F/O molar ratio gives lower particle sizes and this is in good agreement with the size determined by XRD analysis (Table 1). These features could be attributed to the expectedly higher exothermicity associated with higher F/O ratio.

The TEM micrographs of the synthesized Co_3O_4 at F/O 0.5 being calcined at 400 and 1000°C are shown in Fig.10-a and -b, respectively. The TEM micrographs show the nano-crystalline nature of the prepared Co_3O_4 spinel. Fig.10-a, shows that the particles size in the range of 14-16 nm. These results are in a good agreement with the sizes determined from XRD analysis (Table 2). Moreover, the particles of this sample have homogeneous, weak agglomeration and uniform distribution in the powder sample. Inspection of Fig.10 (b) revealed that, thermal treatment of the precursor at elevated temperatures plays a significant role on the variation of particle size and morphology of Co_3O_4 spinel. In this case, it could be seen that the particle size in the range of 28-31 nm, which is again in close agreement with the sizes determined from XRD analysis (Table 2). Particles of Co_3O_4 calcined at elevated temperatures are more agglomerated than that at lower one. As a conclusion, the F/O ratio has clearly important role on the structural and morphological properties of the powders. Low F/O ratios are recommended in this case in order to avoid agglomeration of the particles and to obtain powders with small particle size. Also, products with low calcinations temperatures are recommended for the same reason.

Table 1. Crystallite sizes of Co_3O_4 at different glycine/cobalt nitrate molar ratios being calcined at 400°C

Glycine/ Co^{2+} molar ratio	0.5	1	1.5	2	5	8	16
Crystallite size [nm]	15.3	16.9	17.9	18.4	23.8	21.9	21.9

**Figure 10.** TEM of as-prepared Co_3O_4 at glycine to cobalt molar ratio of 0.5 calcined at, (a) 400°C and (b) 1000°C **Table 2.** Crystallite sizes of Co_3O_4 at glycine/cobalt nitrate molar ratio of 0.5:1 calcined at different calcinations temperature

Calcination temperature	350	400	500	600	700	800	900	1000
Average Crystallite size [nm]	21.6	15.3	15.5	20.7	24	28.2	29.5	28

4. Conclusions

It is well known that combustion synthesis is an efficient, quick, simple, low cost and straightforward method for preparation of nanosized materials at lower temperatures. In this work we have prepared spinel Co_3O_4 employing solution combustion synthesis (SCS) using glycine as a fuel. Glycine content is the key factor that controls the formation of reduced oxidation state compounds such as CoO phase. The ratio of the fuel to nitrates dramatically influenced the phase formation of the final products and the particle size. When the ratio of fuel to nitrates was (1.5-5) the final products were attributed to Co_3O_4 and CoO phases, but at lower (0.5-1) or higher ratios (8-16) the final product were mainly spinel Co_3O_4 phase. The morphology of the as-prepared Co_3O_4 is a hollow nanotubular. The calcined powders showed the presence of regular particles, with narrow particle size distribution. In addition, this methodology can lead the system to a good chemical homogeneity as the reagents were mixed in an aqueous solution.

REFERENCES

- [1] U. Zavyalova, P. Scholz, and B. Ondruschka, *Appl. Catal. A Gen.* 323, 226 (2007)
- [2] B.M. Abu-Zied, S.A. Soliman, *Catal. Lett.* 132, 299 (2009)
- [3] T. Garcia, S. Agouram, J.F. Sánchez-Royo, R. Murillo, A.M. Mastral, A. Aranda, I. Vázquez, A. Dejoz, B. Solsona, *Appl. Catal. A: Gen.* 386, 16 (2010)
- [4] N. Koizumi, S. Suzuki, Y. Ibi, Y. Hayasaka, Y. Hamabe, T. Shindo, M. Yamada, *J. Synchr. Rad.* 19, 74 (2012)
- [5] C.B. Wang, C.C. Lee, J.L. Bi, J.Y. Siang, J.Y. Liu, C.T. Yeh, *Catal. Today.* 146, 76 (2009)
- [6] Y. Yu, T. Takei, H. Ohashi, H. He, X. Zhang, M. Haruta, *J. Catal.* 267, 121 (2009)
- [7] N.M. Deraz, *Mater. Lett.* 57, 914 (2002)
- [8] J. Feng, H.C. Zeng, *Chem. Mater.* 15, 2829 (2003)
- [9] S.M.I. Morsy, S.A. Shaban, A.M. Ibrahim, M.M. Selim, *J. Alloys. Comp.* 486, 83 (2009)

- [10] L. Ren, P. Wang, Y. Han, C. Hu, B. Wei, Chem. Phys. Lett. 476, 78 (2009)
- [11] Y. Teng, S. Yamamoto, Y. Kusano, M. Azuma, Y. Shimakawa, Mater. Lett. 64, 239 (2010)
- [12] A.H. Jayatissa, K. Guo, A.C. Jayasuriya, T. Gupta, Mater. Sci. Eng. B. 144, 69 (2007)
- [13] Y. Zhang, Y. Liu, S. Fu, F. Guo, Y. Qian, Mater. Chem. Phys. 104, 166 (2007)
- [14] Y. You-ping, H. Ke-long, L. Ren-sheng, W. Li-ping, Z. Wen-wen, Z. Ping-min, Trans Nonferrous Met. Soc. China 17, 1082 (2007)
- [15] X. Ke, J. Cao, M. Zheng, Y. Chen, J. Liu, G. Ji, Mater. Lett. 61, 3901 (2007)
- [16] J. Jiang, L. Li, Mater. Lett. 61, 4894 (2007)
- [17] J.C. Toniolo, A.S. Takimi, C.P. Bergmann, Mater. Res. Bull. 45, 672 (2010)
- [18] S.T. Aruna, A.S. Mukasyan, Curr. Opin. Solid state mater. Sci. 12, 44 (2008)
- [19] V. Grover, S.V. Chavan, P.U. Sastry, A.K. Tyagi, J. Alloys. Comp. 457, 498 (2008)
- [20] N.M. Deraz, J. Anal. Appl. Pyrol. 88, 103 (2010)
- [21] B.M. Abu-Zied, Appl. Catal. A. 334, 234 (2008)
- [22] C.H. Yan, Z.G. Xu, F.X. Xheng, Z.M. Wang, L.D. Sun, C.S. Liao, J.T. Jia, Solid State Commun. 111, 287 (1999).
- [23] W.G. Fateley, F.R. Dollish, N.T. McDevitt, F.F. Bentley, *Infrared and Raman Selection Rules for Molecular and Lattice Vibrations: the Correlation Method*, John Wiley and Sons, Inc., New York (1972)